Anal. Chem. **2001,** *73,* 3669−3673

Chemical Plume Tracking. 2. Multiple-Frequency Modulation

Timo Kikas, Petr Janata,† Hiroshi Ishida,‡ and Jiří Janata*

School of Chemistry and Biochemistry, Georgia Institute of Technology, Atlanta, Georgia 30332-0400

The purpose of this research is to estimate the effect of turbulent mixing on the information content in a chemically encoded signal, to investigate the effect of the presence of multiple encoded frequencies, and to evaluate the information contained in the higher harmonics of the coherence spectra. The virtual plume instrument is used to mimic the flow conditions and signal patterns in a real chemical plume. Two-frequency modulation experiments are performed using solenoid valves to introduce concentration plugs of a marker into the carrier flows at certain constant frequencies. In our experiments, the length of the delay elements and the dispersion were varied to mimic different characteristics of the turbulent plume. In addition, an artificial but *uncorrelated* white noise was added to the raw amperometric signals in order to simulate the "noisy" conditions existing in a real plume. Our experiments reveal that the introduced turbulence has only a marginal effect on the coherence spectra. Moreover, it is shown that when the second frequency is present in the plume, both fundamental frequencies can be unambiguously assigned. Higher harmonics in the coherence spectra have been found to depend on the distance from the source. These findings are important for understanding of the mechanism of chemotaxis and may also lead to the design of optimized search algorithms for chemical plume tracking robots.

In the first part of this work,[1] we introduced the methodology of correlation analysis of signals from an amperometric sensor array in a flowing stream, constrained in narrow tubing. It was shown that concentration impulses could be encoded over a relatively broad range of frequencies and read at a distance of over 2 m from the source. A robust correlation parameter in those experiments proved to be the *coherence*, $\alpha^2(\omega)$

$$\alpha(\omega) = \{\text{cross-power spectrum } (\omega)\}_{a,b}{}^2 / \{\text{autopower spectrum } (\omega)\}_a \times \{\text{autopower spectrum } (\omega)\}_b$$

The important attribute of this parameter is the ability to accentuate the correlated and to screen out the uncorrelated parts of the energy in the signal. Thus, the coherence of fully correlated signals detected by a pair of sensors is unity while the coherence of completely uncorrelated signals is zero.

To simulate the real conditions existing in a nonconstrained turbulent plume, dispersion elements were added to the flow and white noise was added to the raw amperometric signal. The dispersion elements cause turbulent dilution of the concentration segments with the carrier solution. Unlike the definition of the dilution as it occurs in flow injection analysis format,[2] the dispersion was defined as the ratio of the peak-to-peak amplitude of the signal from the setup with no dispersion element to the amplitude of the signal with the dispersion element added into the same setup (Figure 1). In the nonconstrained plume, this would correspond to the condition of detecting the chemical marker far from the source when it has been dispersed by numerous random dilution events.

Under the conditions of such defined dispersion, we have further examined the encoding of multiple frequencies and the possibility of estimating the distance of the sensor array from the source by utilizing the behavior of the coherence parameter. Finally, we investigated the effect of switching artifacts that were not related to the concentration modulation but only to the inadvertent modulation of the flow, propagating through the virtual plume apparatus. These artifacts and their elimination are an interesting illustration of the design characteristics of the virtual plume.

EXPERIMENTAL SECTION

Experiments were performed in a controlled benchtop apparatus called the "virtual plume" (VP). The basic elements of the VP and experimental conditions have been described in previous articles.[1,3] The block diagram of the frequency-modulated virtual plume (MVP) for a two-frequency modulation experiment is shown in Figure 2. The basic setup was modified according to specific requirements of the experiments at hand (see experimental descriptions under Results and Discussion). All experiments were done at least in triplicate. Using this setup, we examined the effects of dispersion, distance, and presence of another modulation frequency. We also studied the character of the higher harmonics of the modulation frequencies and their information content.

* Corresponding author: (phone) (404) 894 4828; (fax) (404) 894 8146; (e-mail) jiri.janata@chemistry.gatech.edu.

† Department of Psychological and Brain Sciences, Dartmouth College, Hanover, NH 03755.

‡ Present address: Department of Physical Electronics, Tokyo Institute of Technology, 2-12-1 Ookayama, Meguro-ku, Tokyo 152-8552, Japan.

(1) Kikas, T.; Ishida, H.; Webster, D. R.; Janata, J. *Anal. Chem*. **2000**, *73*, 3662−3668.

(2) Ruzicka, J.; Hansen, E. *Flow Injection Analysis*; J. Wiley & Sons: New York, 1988.

(3) Kikas, T.; Ishida, H.; Roberts, P. J. W.; Webster, D. R.; Janata, J. *Electroanalysis* **2000**, *12*, 974−979

10.1021/ac010391f CCC: $20.00
Published on Web 07/04/2001

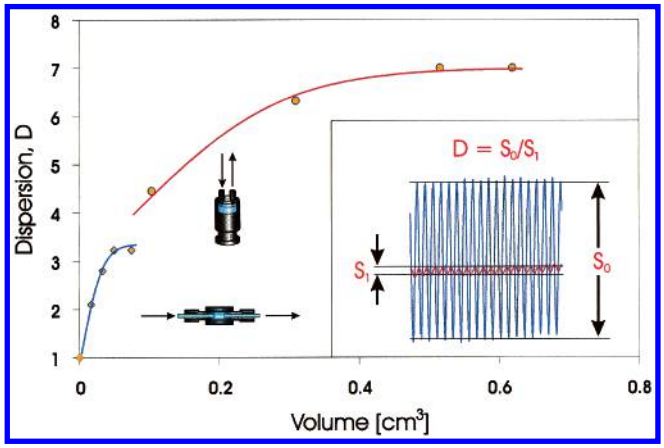

Figure 1. Dependence of the dispersion on the volume and geometry of the dispersion element. Data points represented by squares are acquired using linear dispersion element; data points represented by rings are acquired using nonlinear dispersion element. The inset shows the definition of dispersion *D*. S_0 and S_1 are the amplitudes of the amperometric signal without and with dispersion element, respectively.

To mimic the turbulent nature of a real plume, white noise from a random number generator was added to the time series (raw signal) from the two amperometric sensors. The amount of energy in this added noise is expressed as the percentage of the energy contained in all the frequencies of the concentration modulation at $L = 0$.

The delay elements were designed to provide different retention times for marker plugs while minimizing additional dispersion. Coils of Teflon tubing with inner diameter of 0.5 mm and lengths from 10 to 100 cm were used for this purpose.

The dispersion elements (DiE) were designed to create considerable additional dispersion without additional delay. For small dispersion values, the so-called "linear" dispersion elements, 2−9-mm-long pieces of tubing with bigger inner diameter (3.24 mm) were used. For higher dispersion, elements with a mixing chamber (diameter 9.32 mm) were used (see Figure 1). The latter contain a movable piston to control the mixing volume of the chamber. In this case, the solution exits the chamber after changing its direction by 180°. In the linear dispersion element, solution enters and exits without a change in the flow direction. As expected the mixing chamber yields a higher degree of dispersion (Figure 1).

The sensing elements consist of carbon microelectrodes housed in the flow-through cells. A three-electrode electrochemical configuration was used in order to prevent polarization of the silver wire reference electrode. A stainless steel outlet tube served as an auxiliary electrode (Figure 2).[3]

Solutions and Reagents. An aqueous 0.482 M NaCl solution was used as the carrier solution. A 2.5 mM solution of hexaaminerutheniun trichloride ($(NH_3)_6RuCl_3$) was again used as the electrochemical marker because of its ideal electrochemical behavior.

RESULTS AND DISCUSSION

Effect of the Dispersion on the Coherence Spectra. Up to this point, the flows in our experiments have been nearly laminar and constrained by the walls of the tubing.[1] However, in real chemical plumes, flow is turbulent and unconstrained. To study the effects of the turbulence on the encoded signal, we introduced additional dispersion elements into the VP setup (described above). In the dispersion elements, the flow approaches turbulent because the abrupt change in the diameter of the flow path makes the flow unstable and unconstrained by the wall. The volume of this dispersion element is much greater than the volume of the individual concentration pulse.

To understand the relationship between the dispersion of the marker and the volume of the mixing chamber, signal amplitude of the reference marker with the dispersion element was normalized to the signal amplitude of the marker without the dispersion element. Figure 1 shows that the dispersion initially increases with the volume but later becomes independent of the volume. A nonlinear DiE introduces higher dispersion of the marker due to the increased mixing.

The single-frequency flow modulation experiments were performed using DiEs with various values of dispersion. Coherence values in the frequency domain were determined for the different dispersions, using the data set from the flow modulation experiment with and without the DiE. Figure 3 shows that neither the fundamental frequency nor the coherence value is significantly affected by the dispersion. However, the number of peaks at higher frequencies in the coherence spectrum decreases sharply with increased dispersion.

Information in Higher Harmonics. Looking at the coherence spectra one can see readily that coherence values at higher harmonics often change with changing conditions even though the coherence value at the fundamental frequency itself does not change. This observation raises the possibility that there is additional useful information in the higher harmonics of the modulation frequency. To explore this possibility, we revisited the data from the flow modulation experiments performed previously[1] and plotted the ratio of the coherence at the fundamental frequency and at the first harmonic versus the length of the delay element (L). This was done for two different modulation frequencies. Figure 4 reveals sharply increasing curves beyond some critical length, L_c, which depends on the modulation frequency. Furthermore, a linear trend is observed below L_c. The linear trend is a result of the decrease of the coherence at the first harmonic with the increasing distance from the source, while the coherence value at the fundamental frequency remains constant. Knowing this linear trend allows us to estimate the distance from the source using the coherence ratio. A sharp increase in the coherence ratio occurs when the coherence value at the first harmonic drops below the threshold noise level of 3σ at L_c. Addition of artificial white noise with an intensity of 10% of the original signal intensity increases the $(\text{coherence})_0/(\text{coherence})_1$ ratio, and effectively decreases the critical length (Figure 4). The origin of the effect is due to the fact that the power at the higher harmonics is low. Adding white noise results in increased phase variance at all frequencies. Since the power at the higher harmonics is low, the contribution of phase variance by the noise is proportionately much larger than at lower frequencies. Therefore, coherence at higher frequencies drops dramatically while being less affected at lower frequencies.

Another way to look at the effect of distance is to count the number of higher harmonics present in the frequency spectra above a selected threshold value. For that purpose, the data were

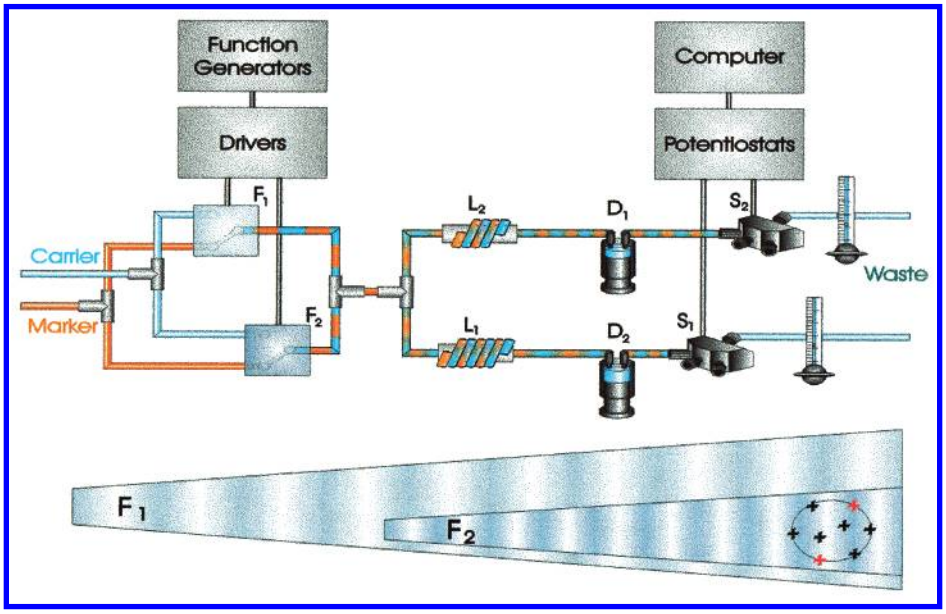

Figure 2. Block schematic of the virtual plume used to study two-frequency modulation. F_1 and F_2 represent frequencies introduced by solenoid valves, L_1 and L_2 represent lengths of the delay elements, D_1 and D_2 represent dispersion elements with two different dispersion values, and S_1 and S_2 represent flow-through amperometric sensors.

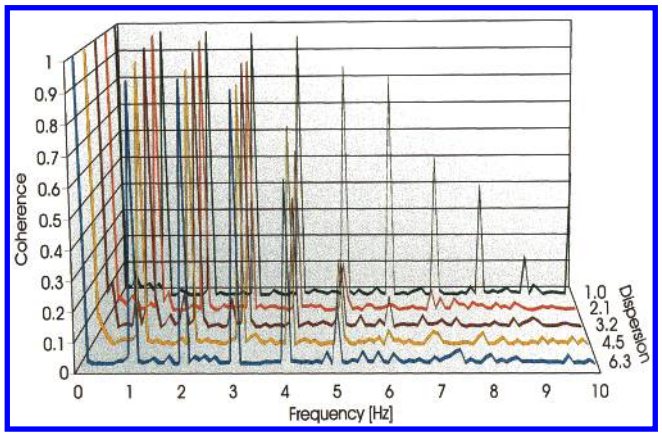

Figure 3. Dependence of the coherence spectra on dispersion. Flow rate in the channels was kept 0.6 mL/min.

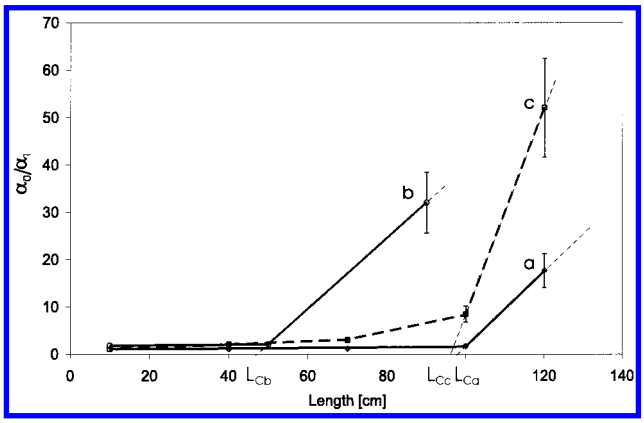

Figure 4. Dependence of the ratio of coherence at the fundamental modulation frequency (α_0) over the coherence at the first harmonic (α_1), on the distance. The fundamental frequencies were (a) 1.0 and (b) 2.5 Hz. The plot c corresponds to data set (a) with 10% white noise added. The experiments were run in triplicate.

collected from frequency modulation experiments with different delay elements (that mimic the distance from the source) while the modulation frequency and the main setup of the VP was the same.[1] The number of coherence peaks at $S/N > 3\sigma$ in the frequency spectra was then plotted against the distance from the modulation source (Figure 5). The number of coherence peaks at higher harmonics of the fundamental frequency (N_L) decreases with the increasing distance, L, according to the empirical relationship

$$N_L = N_0(1 + aL^2 - bL)$$

where N_L is number of peaks present in the coherence spectrum at distance L cm for the source, N_0 is the number of peaks at $L = 0$. The empirical constants ($a = 0.0004$, $b = 0.1282$) have been fitted to our data. The coherence value at the fundamental frequency stays nearly constant up to the critical distance, L_c.[1] The *number* of peaks present in the coherence frequency spectrum is always an integer. It contains even more information about the distance of the array from the source than the coherence value at the fundamental frequency itself. Therefore, the number of harmonics present in the frequency spectrum might prove especially useful when the searcher is in the close proximity of the source.

Encoding of Multiple Frequencies. Real chemical plumes are always subject to many different perturbations originating from physical bodies in the flow path. Therefore, we performed flow modulation experiments with two unique frequencies applied simultaneously according to the schematic shown in Figure 2. The resulting coherence spectra were more complex than those of the single encoded frequency. The most prominent peaks in Figure 6 can be again assigned to the fundamental modulation frequencies, higher harmonics, and their linear combinations. More complex combinations produced peaks comparable to the noise level.

In the special case when one frequency is the harmonic of another frequency, the coherence values add (Figure 7). The

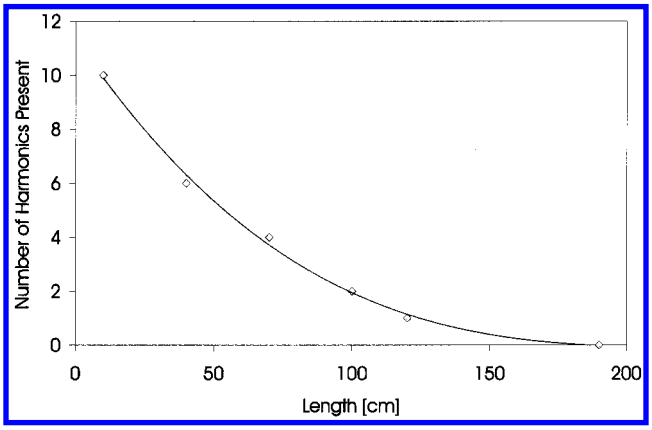

Figure 5. Dependence of the number of peaks at higher harmonics, present in the coherence spectrum on the distance. Modulation frequency was 1 Hz.

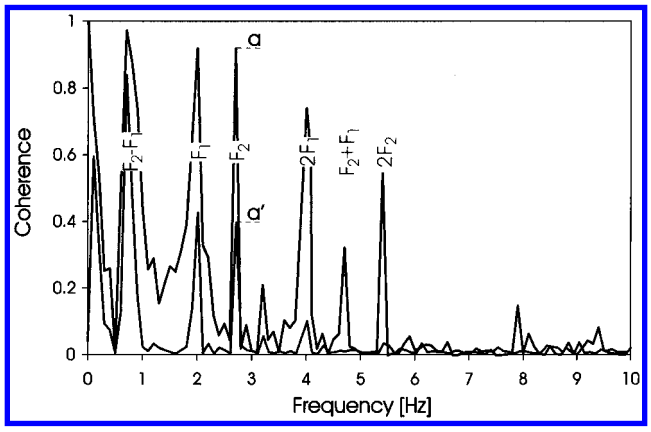

Figure 6. Coherence spectrum obtained with simultaneous two-frequency modulation. The first frequency was $F_1 = 2.0$ Hz and the second was $F_2 = 2.7$ Hz. The spectrum a corresponds to pure modulation; the spectrum a′ is the same experiment with 10% white noise added.

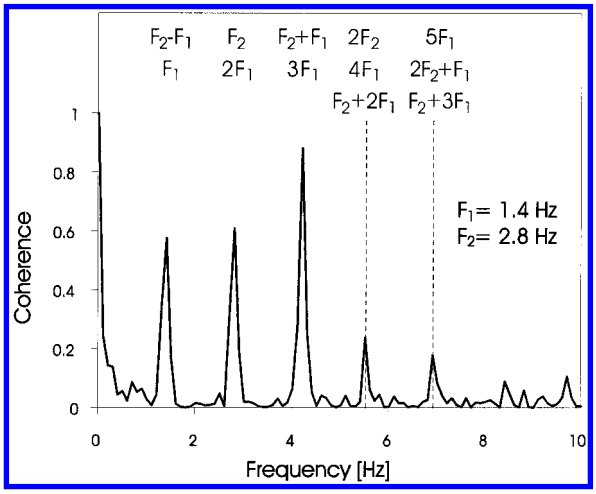

Figure 7. Coherence spectrum of the modulation with harmonic frequencies where F_1 was 1.4 Hz and F_2 was 2.8 Hz.

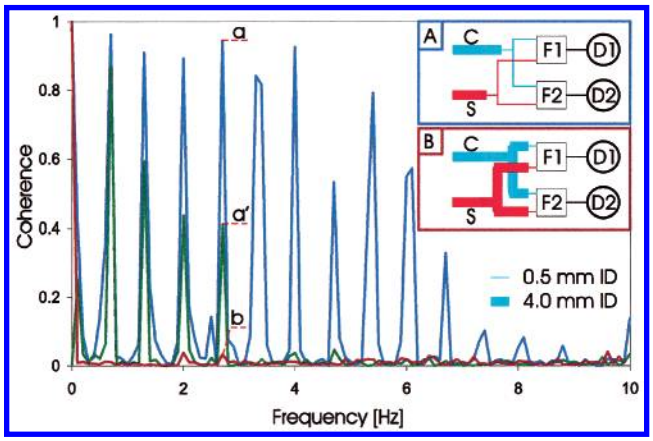

Figure 8. Flow artifact (please see text for explanation). (A) Fluidic setup with narrow T-junctions producing flow artifact (spectrum a). (B) Elimination of the flow artifact by increasing the inner diameter of the channels in the T-junction (spectrum b). Spectrum a′ corresponds to conditions A with 10% white noise added.

reduced noise level and coherence peaks at higher frequencies can be explained by fact that, in this case, all the linear combinations of the fundamental frequencies overlap with the harmonic frequencies. Moreover, this special case cannot be mistaken for a single-frequency case because the intensity patterns of the coherence spectra are quite different: The most intense peak is now at the sum of the fundamental frequencies.

Effect of Dispersion on Two-Frequency Modulation Spectra. Similar experiments of two-frequency signal modulation with the addition of dispersion element (with $D = 7$) were performed to evaluate the effect of dispersion on the coherence spectra. This value of dispersion did not introduce any notable changes. However, introduction of white noise at the 10% level produced noticeable changes shown by spectrum a′ (Figure 6).

From these results, we can predict that addition of more frequencies will generate more complex coherence spectra but the prominent peaks should be readily assignable to fundamental frequencies, higher harmonics, or their linear combinations. Thus, it should be possible to combine this information with our understanding of coherence ratios and to map the flow path of the chemical marker from the source to the array.

Flow Artifact. The following experiments were performed in order to ascertain that the coherence values were caused only by the concentration modulation and not by any other extraneous correlated perturbations. In the first experiment, the background electrolyte "carrier" was introduced into both input lines. Therefore, the concentration of the electroactive "marker" remained zero throughout the switching between these two streams. With only carrier solution in the setup, there was no coherence observed above the noise level. In the second experiment, the two input streams contained identical concentration of the marker, thus resulting in no modulation of the amperometric signal in either channel. With only marker solution in the setup, the coherence spectrum showed two low-intensity peaks, one at the fundamental frequency and another at the first harmonic ($\omega^2 = 0.1$). This artifact can be attributed to the momentary increase of the mass transport to the electrode surface in the instant of switching.

The third, most revealing experiment was performed with the fluidic circuits depicted in Figure 8. In that case, the concentration modulation was done with two frequencies ($F_1 = 2.0$ Hz and $F_2 = 2.7$ Hz), each assigned to only one channel. If the concentration modulation were the only correlatable signal, the coherence values should be zero for the entire spectrum. However, in reality, a strong correlation including higher harmonics was obtained with the fluidic scheme A. On the other hand, no coherence was obtained when the narrow internal diameter tubing (0.5-mm i.d.)

in the T-junctions was replaced with a 4.0-mm-i.d. tubing. The switching artifact was caused by the unintentional modulation of the flow in channel 2 by the solenoid 1 and vice versa. This unwanted modulation represents a cross-talk that affects the coherence values. The fact that it can be eliminated by increasing the internal diameter of the T-junction (Figure 8, scheme B) underscores the importance of careful experimental design. It again illustrates the high sensitivity of the coherence to the presence of the correlated part of the signal. The added uncorrelated white noise significantly reduces the effect of this artifact and, in this case, would have a beneficial effect (Figure 8, spectrum a′).

CONCLUSIONS

The experiments described in parts 1 and 2 of this study confirm that information can be encoded in laminar and turbulent constrained streams, in the form of fluctuating concentration of the chemical marker and decoded in the frequency domain by the sensing array (pair of sensors, in this case). The possibility of using autopower spectral density, cross-power spectral density, and coherence was investigated.[1] The most robust parameter tested for this analysis proved to be coherence, which represents a frequency-specific correlation coefficient.[4,5] Coherence is immune to the variations in average flow velocity. This is a remarkably useful attribute because the local flow velocity cannot be controlled or easily detected in natural plumes. The nonsinusoidal form of the concentration variation leads to the formation of higher harmonics in the frequency analysis. The ratio of the value of the coherence at the fundamental frequency to that at the first harmonic can be used to estimate the distance of the sensor array from the modulation source. This is consistent with the fact that the coherence at higher harmonics decays much faster with the distance than that at the fundamental frequency.

The unconstrained plumes in the natural environment contain a continuous spectrum of frequencies generated by objects of various dimensions and shapes in the flow.[6] These could be, for example, stones in the riverbed. They represent multiple-frequency noise, parts of which could be correlated. It is the nature of the coherence function that the uncorrelated signals would be rejected. The possibility of encoding/decoding multiple frequencies was therefore investigated in our virtual plume both in the presence and in the absence of uncorrelated noise. The resulting coherence spectra contained multiple, well-resolved peaks that could be unambiguously assigned to linear combinations of the fundamental frequencies and their harmonics. This result again confirms the robustness of coherence and its significance for information transmission.

The results with the virtual plume show great promise for elucidating the fundamental elements of chemotaxis. They need to be confirmed by other methods, e.g., laser-induced fluorescence or in situ measurements from an amperometric array placed in an unconstrained plume. Nevertheless, the probability that coherence will emerge as a new parameter for chemical plume tracking is very high. Our study also reveals a new aspect of sensing with arrays of chemical sensors that hitherto has not been recognized. The correlation analysis of signals received from the sensor array opens the possibility of extracting the spatial information about the location of the source of the chemical signal. The significance of this finding for location of point sources of chemical pollution is obvious. Such information would be sufficient as the basis of navigation system for man-made tracking robots that could be used for any environmental remediation. The conditions existing in the far field of a real plume can be simulated by increasing the relative contribution from the random noise. In the limit, the relative energy in the fluctuation-encoded signal would become negligible. In that case, only the nonzero *mean* value of the concentration, if detectable, would inform the searcher that it is in the "correct neighborhood" but would not provide another meaningful navigational cue.

Perhaps even more intriguing is the possibility of establishing a link between the frequency spectrum of the signal and the search behavior of aquatic animals. It should not be forgotten that the present results have been generated by only *one pair* of chemical sensors. Thus, the coherence resulting from this analysis is only a one-dimensional vector. The obvious drawback is the length of time (∼1000 s) needed to acquire the data for Fourier transform analysis. The marine animals possess four or more pairs of chemical sensors or sensor groupings that may result in much faster acquisition of the navigational information. It is therefore intriguing to speculate that the correlation analysis in the multidimensional vector space would be performed according to a much more efficient algorithm resulting in a drastically reduced evaluation time.

(4) Bendat, J. S.; Piersol, A. G. *Random Data: Analysis and Measurement Procedures*; J. Wiley & Sons: New York, 2000.
(5) Hartmann, W. M. *Signals Sound, and Sensation*; Springer-Verlag: New York, 1998.
(6) Tennekes, H.; Lumley, J. L. *A First Course in Turbulence*; MIT Press: Boston, MA, 1972.

ACKNOWLEDGMENT

The authors acknowledge helpful discussions and comments in the area of animal physiology and behavior (M.J. Weissburg, D.B. Dusenbery) and fluid mechanics (D.R. Webster, P.J.W. Roberts). The support for this work has been provided by DARPA/ONR Project N00014-98-1-0776.

Received for review April 5, 2001. Accepted June 4, 2001.

AC010391F